
STRENGTH AND PLASTICITY

Measurement of Young's Modulus and Hardness of Al–50 wt % Sn Alloy Phases using Nanoindentation

O. A. Chikova^a, E. V. Shishkina^a, and A. N. Konstantinov^b

^a*Yeltsin' Ural Federal University, ul. Mira 19, Ekaterinburg, 620002 Russia*

^b*Ural State Pedagogical University, ul. Mashinostroitelei 11, Ekaterinburg, 620083 Russia*

e-mail: chik63@mail.ru

Received September 5, 2012; in final form January 9, 2013

Abstract—The nanoindentation method was used to measure the Young's modulus and hardness of the phases of the alloy Al–50 wt % Sn: α -aluminum and eutectic. Samples are obtained in different ways, i.e., traditionally via the transition of the melt into a homogeneous structural state by heating to a certain temperature, followed by cooling using the cooling rate greater by the order than that of the traditional method and via the addition of 0.06 wt % Ti and 1 wt % Zr to the binary alloy. It has been found that the most significant effect of the Al–50 wt % Sn phases on the Young's modulus is the transition of the melt into a homogeneous structural state and the introduction of Zr into the melt. As part of the mathematical theory of elasticity, a numerical evaluation of the interfacial pressure that arises due to the difference between Young's modulus of α aluminum and eutectic has been performed. The calculation has showed that the extra pressure is nine times less for the alloy formed through the transition of the melt into a homogeneous structural state than for the alloy produced via a traditional way.

Keywords: Young's modulus, hardness, nanoindentation

DOI: 10.1134/S0031918X1307003X

1. INTRODUCTION

The mechanical properties of crystalline materials, in particular metal ones, depend on how these materials are produced. It is known that the transition of the melt into a homogeneous structural state, which takes place by heating it to a temperature specific to each composition, as well as increasing the cooling rate of the liquid metal and introducing alloying elements into it, affects the mechanical properties of the ingot [1]. In particular, we have shown that the heat treatment of Al–Si melts, which provides a transition of the melt into a homogeneous structural state, leads to an increase in the plasticity of the cast metal 10–15 times and the strength, by 30–80% [2]. We know that the transition of a liquid metal into a homogeneous structural state by heating to a desired temperature changes the microhardness of the phases of the ingot during subsequent cooling and solidification [1]. The relationship between the microhardness and other mechanical properties should be noted. In fact, indentation and scratch hardness tests can provide almost the same information about the properties of metals as tension does [3]. We do not know of studies on the influence of the production technique of an ingot on its Young's modulus, plasticity, and the 0.2 offset yield strength of its phases. The dependence of the mechanical characteristics of the ingot on those of its phases is poorly understood, since it requires mechanical testing in microvolumes.

The nanoindentation method makes it possible to conduct mechanical tests in microvolumes and to experimentally determine the Young's modulus E and the hardness H of individual phases of the ingot [4]. The nanoindentation method is based on the measurement and analysis of the dependence of the surface indentation load P on the indenter penetration depth h . This method is nondestructive and allows one to correctly measure the Young's modulus in the range of absolute values of 50–1000 GPa. The minimum size of an area where measurements are carried out is on the order of 200 nm.

Al–Sn alloys are known for their antifriction properties and meet the Charpy principle [9], they are used as a material for the manufacture of bearings and sliding supports. The aim of this work is to measure the Young's modulus and the hardness of the phases of the Al–50 wt % Sn cast alloy. The experimental Young's modulus values of the Al–50 wt % Sn phases present in a tin solid solution in aluminum and eutectic will allow us to estimate the compressibility of the ingot, which is important for choosing a manufacturing method.

2. EXPERIMENTAL

The phase diagram of the Al–Sn system is of eutectic type. Al–Sn alloys are characterized by a tendency

to separate into two phases, i.e., tin solution in aluminum and eutectic. The eutectic point occurs at a content of 97.8 at % Sn at 228.3°C [5, 6]. The microstructure of the Al–50 wt % Sn (18.5 at % Sn) alloy includes dendritic α -solid-solution grains surrounded by eutectic Sn–Al layers (Fig. 1).

Samples to be investigated were obtained in various ways: a traditional one, a transition of the melt into a homogeneous structural state by heating to a certain temperature, followed by cooling using an order-greater cooling rate, and the addition of 0.06 wt % Ti and 1 wt % Zr to the binary alloy. Previously, it was established from viscometric tests that the Al–50 wt % Sn melt must be heated above 950°C [7, 8] in order to make it pass into a homogeneous structural state. Traditionally, the heating temperature of the Al–50 wt % Sn melt does not exceed 700°C and its cooling rate in solidification is about 0.1 K/s. In this research, we increased the heating temperature of the melt to 1150°C and the cooling rate of the metal to 4 K/s. The studies were conducted to study the influences of the production technique on the mechanical properties of the individual phases of the ingot.

The Al–50 wt % Sn samples were melted from pure tin of OVCh000 grade and aluminum of A999 grade in laboratory conditions. Before the Young's modulus and hardness tests, sample surfaces were first mechanically polished and then electrochemically treated to minimize a roughness height to ~10 nm.

The Young's modulus and hardness of the Al–50 wt % Sn alloy phases were measured using an NTEGRA Probe Laboratory nanosclerometric module (NT-MDT, Zelenograd, Russia). The measurements were carried out under load ramp, with continuous loading at room temperature. The indenter imprints were analyzed to determine the Meyer hardness HM (GPa) and the Young's modulus E (GPa) of the phases of the ingot that are a tin solid solution in aluminum and eutectic. The elastic component of strain was estimated by the formula

$$r = \frac{h_m - h_f}{h_m} \times 100\%, \text{ where } h_m \text{ is the maximum depth}$$

of indentation and h_f is the impression depth after unloading. An analysis of the imprints was carried out when selecting the parameters of the power function. The function describes the experimental dependence of the depth of indentation on the applied load and the dependence of the contact area on the applied load. The Young's modulus measurement method, which is implemented in the nanosclerometric module of the NTEGRA Probe Nanolaboratory, is based on the use of a piezoresonance probe sensor with a fork construction with high bending resistance ($\sim 10^4$ N/m), which allows one to use probes with 1000 times more rigidity than regular AFM probes. In the context of the method, it is possible to map the surface distribution of the elasticity modulus, i.e., to obtain images for which the contrast is based on differences in the local

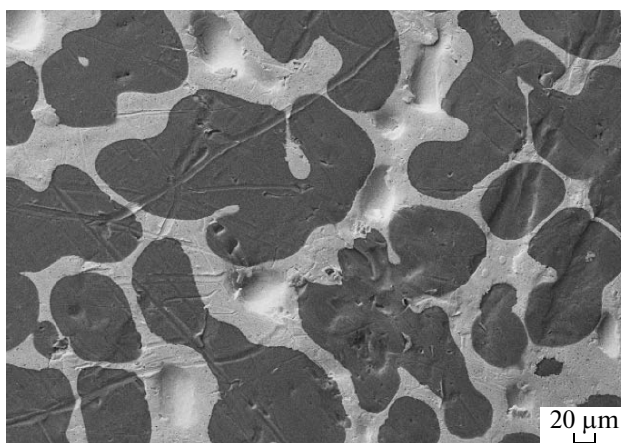


Fig. 1. Microstructure of Al–50 wt % Sn alloy. Sample was prepared at an elevated heating temperature of 1150°C and the cooling rate $v_{\text{cool}} = 0.2$ K/s.

Young's modulus E . The original design and operation of the probe makes it possible to distinguish the tough and elastic components of the interaction forces between the probe tip and a surface. This feature allows one to indicate a solid surface beneath a viscous adsorbed layer and perform measurements in open air without any special preparation of the sample.

Before the indentation, a selected area of the sample surface was scanned to ensure that the sample surface was smooth and no defects would affect the measurements and choose the imprint location. The load applied to the indenter increased monotonically from 0.25 to 2.50 mN. The indentation resulted in the dependence of the applied load on the probe coordinates for each imprint. The nanosclerometric module was calibrated using a plate that was manufactured from fused silica with known values of the Young modulus and hardness. In the experiments, a Probe B-S-10-NOVA probe was used, in which a Berkovich diamond triangular prism served as the working part. The indenter imprints were measured via the results of sc-SPM (semi-contact scanning probe microscopy). The Young's modulus and hardness of the phases were determined after 15 measurements. Measurement errors were estimated by conventional methods [10] at a confidence probability of 95%.

The crystal structure and elemental composition of the phases were examined by conventional metallography methods using an Auriga CrossBeam workstation. A focused ion beam was used for additional sample preparation and X-ray microanalysis (EDS) to determine the elemental phase composition. The etching mode of the surface of the samples was 30 kV, 16 nA, and $\tau = 2$ min. The investigations were performed in the Morden Nanotechnologies Center for Collective Use of the Institute of Natural Sciences of Ural Federal University.

Young's modulus and hardness of phases of Al–50 wt % Sn alloy

Production technique of a sample	Eutectic			Sn solid solution in Al		
	<i>r</i> , %	<i>E</i> , GPa	<i>H</i> , GPa	<i>r</i> , %	<i>E</i> , GPa	<i>HM</i> , GPa
$T_h = 700^\circ\text{C}$ $v_{\text{cool}} = 0.2$ K/s	—	97.93 ± 4.93	0.51 ± 0.06	3.3	68.88 ± 5.10	0.73 ± 0.07
$T_h = 1150^\circ\text{C}$ $v_{\text{cool}} = 0.2$ K/s	0.8	55.37 ± 1.81	0.52 ± 0.04	6.8	49.24 ± 3.01	0.62 ± 0.03
$T_h = 700^\circ\text{C}$ $v_{\text{cool}} = 4$ K/s	—	100.73 ± 4.19	0.56 ± 0.01	3.7	68.89 ± 1.10	0.66 ± 0.02
$T_h = 1150^\circ\text{C}$ $v_{\text{cool}} = 4$ K/s	2.3	45.22 ± 1.61	0.65 ± 0.02	7.6	36.56 ± 0.47	0.69 ± 0.03
$T_h = 1150^\circ\text{C}$ $v_{\text{cool}} = 4$ K/s Al–50 wt % Sn–0.06 wt % Ti	—	57.26 ± 3.10	0.55 ± 0.06	13.7	68.57 ± 11.59	0.73 ± 0.07
$T_h = 1150^\circ\text{C}$ $v_{\text{cool}} = 4$ K/s Al–50 wt % Sn–1 wt % Zr	7.6	35.31 ± 5.93	0.57 ± 0.05	7.8	39.28 ± 1.76	0.63 ± 0.06

3. RESULTS

The measured results of the Young's modulus and the hardness of the Al–50% Sn phases are summarized in the table. It was found that the transition of the melt into a homogeneous structural state by heating up to 1150°C with subsequent cooling and solidification at a rate $v_{\text{cool}} = 0.2$ K/s has a significant impact on the Young's modulus value *E* of both an Sn solid solution in Al and the eutectic. The Young's modulus values for the α solution decreased by 30% and that for the eutectic decreased by 44%; i.e., the Young's moduli of the phases differ from each other by 12%, rather than 42%. The hardness of the Sn solid solution in Al decreased by 13% and the hardness of the eutectic remained almost the same. It should be noted that the formation of coarser α -solution dendrites (Fig. 2) during solidification is characteristic of the Al–50 wt % Sn alloy heated in the liquid state up to 1150°C .

An increase in the cooling rate of the metal by an order of magnitude during solidification had almost no effect on the Young's modulus and hardness values of the phases, although significantly changed the microstructure of the alloy: the characteristic α -solution dendrite size decreased by about half at their constant volume fraction and the structure became finer (Fig. 2).

For the transition of the melt into a homogeneous structural state, the combination of heating to 1150°C and a high rate of cooling during solidification enhanced the above effect, which consisted in reducing the Young's moduli of both phases against a background of a slight increase in their hardnesses. The Young's modulus value of the α solution decreased by 48% and that of the eutectic by 53%. The characteristic size of α solution dendrites did not change as the heating temperature of the liquid metal increased to 1150°C (Fig. 2).

The introduction of 0.06 wt % Ti into the liquid metal at $v_{\text{cool}} = 4$ K/s and a heating temperature of the melt $T_h = 1150^\circ\text{C}$ hardly changed the Young's modulus and hardness of the α solution dendrites, but it reduced the Young's modulus of the eutectic by 41%

(as compared to a sample obtained at $T_h = 700^\circ\text{C}$ and $v_{\text{cool}} = 0.2$ K/s). In this case, the largest fraction of the elastic component $r = 14\%$ is characteristic of the Sn solid solution in Al. The characteristic size of α solid solution dendrites changed insignificantly.

The introduction of 1 wt % Zr into the liquid metal at $v_{\text{cool}} = 4$ K/s and the heating temperature of the melt $T_h = 1150^\circ\text{C}$ changed the Young's modulus and hardness of both α solution and eutectic most significantly. In comparison with the sample obtained at $T_h = 700^\circ\text{C}$ and $v_{\text{cool}} = 0.2$ K/s, the Young's modulus of the solid solution of Sn in Al decreased by 43% and the eutectic decreased by 64%, while the hardness of the α solution decreased by 14% and the hardness of the eutectic increased by 14%. In this case, the difference between the values of the Young's modulus and hardness of the phases is only 10%. One should note that the fraction of the elastic component of a local strain is almost the same, i.e., 8%, for both phases. The characteristic size of α -solid-solution dendrites changed slightly as compared to the sample obtained at $T_h = 700^\circ\text{C}$ and $v_{\text{cool}} = 0.2$ K/s (Fig. 2).

The X-ray microanalysis (EDS) study of the elemental phase composition of Al–50 wt % Sn samples obtained in different ways showed the presence of aluminum in the amount of 1 wt % in the eutectic (traditional way), 0.5 wt % (melt transition into a homogeneous state), and 0.2 wt % (the addition of titanium). The combination of the transition of the melt into a homogeneous state with an increased rate of cooling in solidification did not change the elemental composition of the eutectic. The Al– α phase of the sample doped with titanium contains Ti in an increased amount relative to the alloy matrix. No titanium was detected in the eutectic interlayers.

Using electron back-scattered diffraction (EBSD), the study of the crystal structure of Al– α dendrites in Al–50 wt % Sn samples prepared traditionally and via the transition of the melt to a homogeneous state has shown that they have a subgrain structure. Several subgrains have a size of about one micron. The comparative analysis of histograms of angle misorientations revealed a large number of large-angle boundaries for

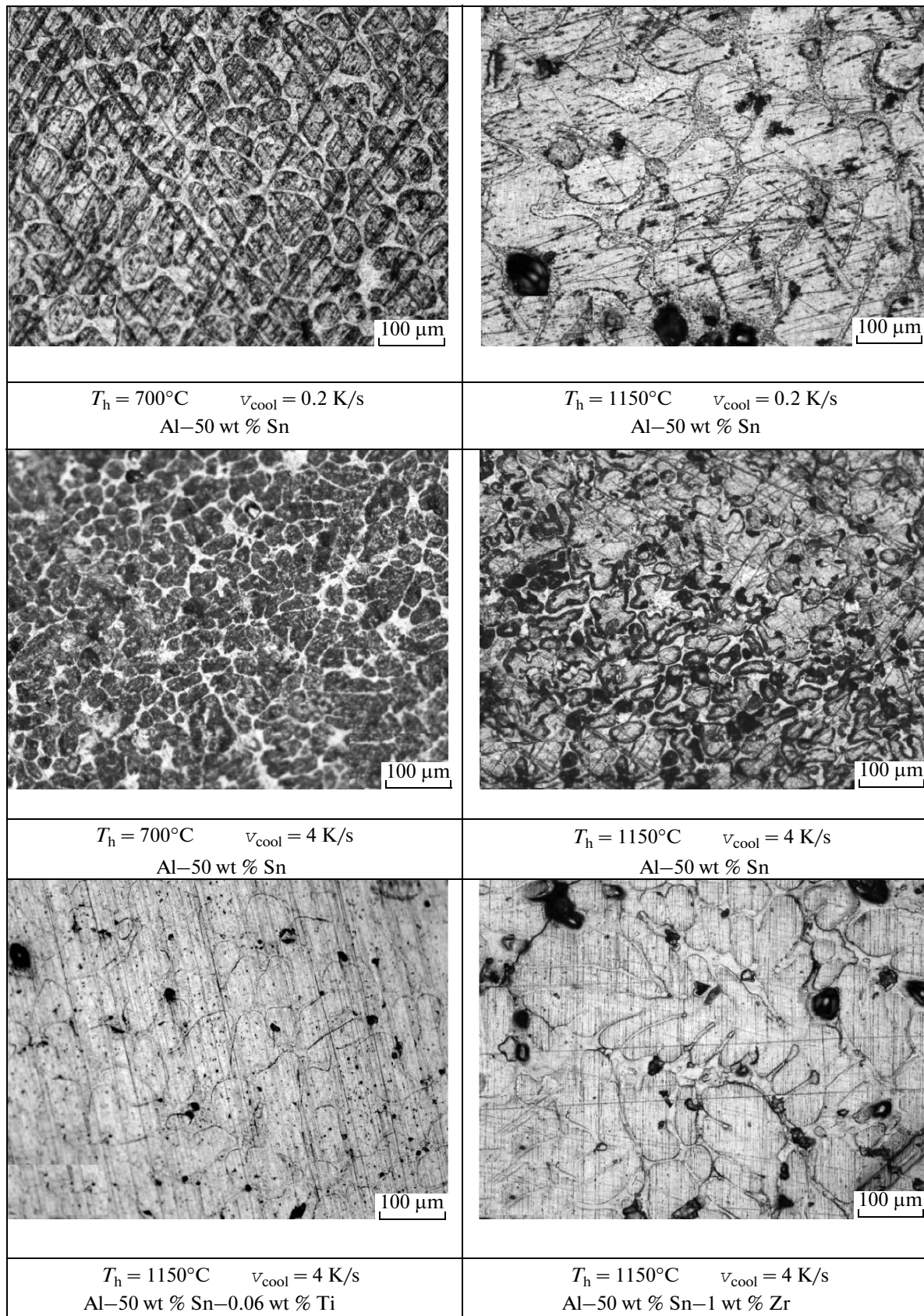


Fig. 2. Microstructures of the Al-50 wt % Sn alloys produced in different ways.

the sample obtained traditionally and almost all low-angle boundaries and the high texture state of the material for the sample prepared via the transition of the melt into a homogeneous state.

Additionally, the strain regimes of the individual phases were studied based on the results of mechanical tests in submicron volumes (nanoindentation) using the load–depth curves (P – h); in particular, we observed a transition from the stable to unstable plastic flow. Al–Sn alloys are classic examples of materials that may exhibit various modes of instability of plastic flow during deformation, in particular the Portevin–Le Chatelier effect [11]. Under the investigation of the traditionally produced alloy, the P – h chart for the α solution showed the first-order steps under loading [11]. First-order steps on the P – h chart were also observed when loading the eutectic in all samples except one containing Ti. The first-order random steps seem to appear due to the formation and evolution of slip bands.

4. DISCUSSION

We have estimated the resulting mechanical stresses, which are dictated by the two-phase state of the Al–50 wt % Sn sample (Fig. 1), i.e., eutectic and α -Al. There is an additional pressure caused by the difference in the elastic moduli between the matrix and inclusions during the deformation of the two-phase sample as follows:

$$P_r = \frac{4\varepsilon\mu\mu_0}{R(2\mu_0 + \mu(\chi_0 - 1))},$$

where $\varepsilon = \frac{F}{4\pi R^2} \left(\frac{1}{E_1} - \frac{1}{E_2} \right)$; $\chi_0 = \frac{\lambda_0 + 3\mu_0}{\lambda_0 + \mu_0}$; $\lambda = c_{12}$ and $\mu = c_{44}$ are the Lamé parameters for a cubic lattice; R is the radius of an inclusion; and F is the external force. The index “0” refers to the characteristics of the inclusion [12].

The calculations have shown that the extra pressure caused by the difference in the elastic moduli between the matrix and inclusions in the alloy prepared by the melt transition into a homogeneous structural state is nine times lower than that in the alloy prepared by the traditional method. On the contrary, an increase in the cooling rate to 4 K/s raises the additional pressure by a factor of 6.5. The same situation is observed, even after preliminary melt transition into a homogeneous structural state, i.e., a 4.6-fold pressure increase. The addition of titanium somehow improves the situation, i.e., the additional pressure decreases 1.5 times as compared to the sample prepared traditionally, and 3 times when alloying the sample with zirconium. We suggest that this additional pressure caused the destruction of samples during rolling [13]. Previously, we found that the transition of the Al–50 wt % Sn melt into a homogeneous structural state using heating to 950°C, followed by cooling and solidification, eliminates the

metal layering in water-cooled rolling. In [13], the above impact of the transition of the Al–50 wt % Sn melt into a homogeneous structural state to improve the workability of the ingot by pressure was explained by changes in the morphology of phases. It has been noted that this melt transition leads to a significant change in the solidification process and results in the formation of a microstructure similar to a modified one [1].

The logical question concerning the nature of the relationship between the change in the Young’s modulus of the phases and the melt transition into a homogeneous structural state arises. According to [1], the transition of the melt into a homogeneous structural state can lead to the supersaturation of an α solid solution with tin.

We know from [14, 15] that a change in the Young’s modulus during alloying is caused by the electronic and size factors. A tin dopant reduces the concentration of electrons in the lattice of the base metal, aluminum [5] and, hence, reduces the kinetic energy of itinerant electrons. A reduction in the kinetic energy of electrons as compared to the whole crystal energy should be accompanied by an increase in interatomic bonds, i.e., an increase in bonding strength. The atomic radius of tin is significantly larger than that of aluminum, which leads to the local deformation of the crystal lattice. Atoms of the matrix will be closer to each other in at least the first two coordination spheres as compared to those in the undeformed crystal. This leads to the appearance of local pressure, which causes an increase in the Debye temperature and elastic modulus. We know the relationship between bonding strength (elastic constants c_{11} , c_{12} , and c_{44} for crystals of cubic symmetry) and the fraction of the kinetic energy of itinerant electrons in the overall energy balance [14, 15]. The substitution of tin atoms for aluminum atoms in the α solution leads to an increase in the elastic moduli c_{11} , c_{12} , and c_{44} and, correspondingly, to an increase in the Young’s modulus of the α -aluminum single crystal $E = \{c_{44}(3c_{12} + 2c_{44})\}/(c_{12} + c_{44})$. The experiment has shown that the transition of the Al–50 wt % Sn melt into a homogeneous state causes a decrease in Young’s modulus of the solid phases of the alloy, which indicates the absence of the phenomenon of supersaturation of α -aluminum solid solution with tin. X-ray microanalysis (EDS) study of the elemental composition of the Al–50 wt% Sn phases also showed no supersaturation of the α solid solution with tin.

Following [1], the melt transition into a homogeneous structural state can also lead to a change in the characteristics of the subgrain structure of α -solid-solution dendrites. The impact of crystallite orientations on the interatomic distance changes the Young’s modulus [14, 15]. According to [14], the presence of only an α -aluminum subgrain structure may change the Young’s modulus by more than 10%. Thus, this factor can not stimulate significant changes in E similar to those reported in this study (see the table).

The authors suggest that grain boundaries and triple junctions play a decisive role in the change of the Young's modulus of the α -solid-solution dendrites and eutectic. In this case, a large fraction of atoms is found at a location other than their normal position in the crystal lattice; the volume fraction of grain boundaries, near-boundary volumes, and triple junctions increases as the subgrain size decreases [16]. For example, according to Mughrabi's composite model [17], the Young modulus can be decreased by increasing the volume fraction of intergranular space, including grain boundaries and triple junctions, the mechanical properties of which are different from those of a grain body. In addition, a decrease in grain sizes increases the proportion of the free volume within the grain boundaries, near-boundary regions, and triple junctions, which is accompanied by a weakening of the atomic bonds in the material. The studies [18–19] suggest a decrease in the strength of microcrystalline materials with decreasing sample thickness below a certain value depending on the crystallite sizes. It was found that, if the ratio of the transverse sample size to the grain size is less than three, then there is a minimum on a yield strength–sample size curve. The minimum is a result of growth in the number of near-surface grains, which have little resistance to plastic deformation due to the dislocation outflow through the external sample surface [18–19]. The characteristics of grain boundaries must have a significant effect on the experimental results, taking into consideration the fact that the imprint size in our nanoindentation tests is about 1–2 mm and corresponds in size to the size of subgrains. Attention is drawn to the fact that the transition of the melt to a homogeneous state upon cooling and solidification has resulted in that almost all boundaries of α -Al subgrains are found to be low-angle and have a significantly higher texture state of the material. Dendrites in the α -Al sample obtained via the transition of the melt to a homogeneous state are similar to single crystals with low-angle boundaries. Thus, the change in Young's modulus of the Al–50 wt % Sn phases formed during the transition of the melt to a homogeneous structural state can be explained by the change in subgrain structure. In particular, the transition of Al–50 wt % Sn into a homogeneous structural state via cooling and solidification leads to the formation of the high texturing structure with α -Al dendrites, where all of the subgrain boundaries are low-angle.

Let us separately discuss the findings on the effect of the production method of the Al–50 wt % Sn alloys on the hardness of α -Al and eutectic phases. In the Oliver and Farr method, we used Meyer hardness HM , which is the average contact pressure to an indenter–sample surface and well agrees with the flow stress [21–23]. The measured hardness of the phase constituents of the Al–50 wt % Sn alloy is consistent with data of the authors of [24].

A crucial point in the discussion of the measurement of Young's modulus and hardness by the Oliver and Farr method is the correlation between the values of these properties. Taking into account the analysis from [23] and using the relationship between c_{11} , c_{12} , and c_{44} elastic moduli and the Young's modulus for fcc crystals in the harmonic approximation [25], it is easy to obtain the calibration dependence between indicators of the indentation chart and mechanical properties of the material in the form of the indentation equation $HM \approx \left(\frac{1}{r} - 1\right)$. The equation suggests that the more elastic the recovery r , the lower the hardness. Thus, the values of HM and r are in agreement with each other. The analysis of the experimental results listed in the table shows that this relationship holds.

5. CONCLUSIONS

(1) The Young's modulus and hardness of the structural constituents of Al–50 wt % Sn (18.5 at % Sn) alloys (the tin solid solution in aluminum and eutectic) produced by different techniques were measured using the nanoindentation method. The effect of the melt homogeneity degree prior to solidification, of the cooling rate of the metal, and of titanium and zirconium additives on the Young's modulus and hardness values of the phases was studied.

(2) The most significant decrease in the Young's modulus of the Al–50 wt % Sn phases was found to be after the melt transition into a homogeneous state via heating to temperatures above 950°C and the introduction of Zr into the melt.

(3) The calculation has shown that the extra pressure caused by the difference in the Young's moduli of the α solid solution and eutectic for the Al–50 wt % Sn alloy passed into a homogeneous structural state from the melt is nine times lower than that for a traditionally prepared alloy. On the contrary, an increase in the cooling rate of the metal from 0.2 to 4 K/s during solidification leads to an additional increase in pressure by the factor of 6.5. An increase in the additional pressure by 4.6 times is observed if the production technique of the Al–50 wt % Sn ingot includes both transition into a homogeneous structural state and an increase in the cooling rate. Titanium and zirconium additives reduce the pressure but insignificantly. It is the extra pressure that is the cause of the destruction of Al–50 wt % Sn alloys in rolling.

(4) The transition of the Al–50 wt % Sn melt into a homogeneous structural state leads to a significant change in the solidification process and microstructure formation of the ingot with other mechanical characteristics of its phases. The changed Young's modulus and hardness values of the α solid solution is experimentally shown to agree with its changed crystal structure. Despite the traditional method of production, where the ingot contains a large number of large-

angle boundaries, the transition of the melt into a homogeneous structural state results in the formation of low-angle boundaries and higher texture state of the material.

(5) The transition of the Al–50 wt % Sn melt into a homogeneous structural state via heating to a temperature above 950°C is the most promising way to improve the workability of the ingot by pressure.

REFERENCES

1. I. G. Brodova, P. S. Popel', N. M. Barbin, and N. A. Vatolin, *Initial Melts as the Basis of Formation of Structure and Properties of Aluminum Alloys* (Ural. Otd. Ross. Akad. Nauk, Ekaterinburg, 2005) [in Russian].
2. D. K. Lykasov and O. A. Chikova, "Optimization of the technology of alloying of the 2124 alloy by manganese on the basis of studying the connection of structure and properties of liquid and cast metal," *Raspilav*, No. 1, 31–39 (2009).
3. M. P. Markovets, *Determination of Mechanical Properties of Metals from Hardness* (Mashinostroenie, Moscow, 1979) [in Russian].
4. Yu. I. Golovin, "Nanoindentation and mechanical properties of solids in submicrovolumes, thin near-surface layers, and films: A review," *Phys. Solid State* **50**, 2205–2236 (2008).
5. L. F. Mondolfo, *Aluminum Alloys: Structure and Properties* (Butterworth, London, 1976; Metallurgiya, Moscow, 1979).
6. *Phase Diagrams of Binary Metal Systems: A Handbook*, Ed. by N. P. Lyakishev (Mashinostroenie, Moscow, 1996), Vol. 1 [in Russian].
7. P. S. Popel and O. A. Korzhavina (Chikova), "Region of existence of metastable microheterogeneity in Al–Sn melts," *Zh. Fiz. Khim.* **63**, 838–841 (1989).
8. O. A. Korzhavina (Chikova) and P. S. Popel, "Viscosity of Al–Sn melts," *Raspilav*, No. 5, 116–119 (1989).
9. Yu. S. Avraamov, I. A. Kravchenkova, and A. D. Shlyapin, "New Al-based antifriction alloys," *Fiz. Khim. Obrab. Mater.*, No. 2, 85–88 (2010).
10. A. N. Zaidel, *Errors in Measurements of Physical Values: A Textbook* (Lan', St. Petersburg, 2005) [in Russian].
11. Yu. I. Golovin, V. I. Ivolgin, M. A. Lebedkin, and D. A. Sergunin, "Regions of the existence of the Portevin–le Chatelier effect under the conditions of continuous room-temperature indentation of an Al–2.7% Mg alloy," *Phys. Solid State* **46**, 1671–1673 (2004).
12. N. I. Muskhelishvili, *Some Basic Problems of the Elasticity Theory* (Nauka, Moscow, 1966) [in Russian].
13. P. S. Popel, O. A. Korzhavina (Chikova), L. V. Mokeva, "Effect of temperature treatment of Al–Sn melt on the structure and properties of cast metal," *Tekhnol. Legk. Splavov*, No. 4, 87–91 (1989).
14. H. B. Huntington, "Elastic Constants of Crystals," in *Solid State Physics* **7**, 214–353 (1958) [*Usp. Fiz. Nauk* **74** (3), 461–520 (1961)].
15. I. N. Frantsevich, F. F. Voronov, and S. A. Bakuta, *Elastic Constants and Elasticity Modules of Metals and Non-Metals. A Handbook* (Naukova Dumka, Kiev, 1982) [in Russian].
16. A. I. Yurkova, A. V. Bilotsky, A. V. Byakova, and Yu. V. Milman, "Mechanical properties of nanostructured iron produced by severe plastic deformation by friction," *Nanosistemy, Nanomaterialy, Nanotekhnologii* **7**, 619–632 (2009).
17. S. P. Nikanorov and B. K. Kardashev, *Elasticity and Dislocation Anelasticity of Crystals* (Nauka, Moscow, 1985) [in Russian].
18. G. A. Malygin, "Influence of the transverse size of samples with micro- and nano-grained structures on the yield and flow stresses," *Phys. Solid State* **54**, 559–567 (2012).
19. G. A. Malygin, "Plasticity and Strength of Micro- and Nanocrystalline Materials," *Phys. Solid State* **49**, 1013–1033 (2007).
20. S. A. Golovin, A. Pushkar, and D. M. Levin, *Elastic and Damping Properties of Structural Metallic Materials* (Metallurgiya, Moscow, 1987) [in Russian].
21. Yu. I. Golovin, *Nano-Indentation and Its Possibilities* (Moscow, Mashinostroenie, 2009) [in Russian].
22. K. V. Gogolinskii, N. A. L'vova, and A. S. Useinov, "Application of scanning probe microscopes and nano-hardness meters for studying mechanical properties of solid materials at a nanolevel (Review)," *Zavod. Labor. Diagn. Mater.* **73**, No. 6, 28–36 (2007).
23. V. F. Gorbun', E. P. Pechkovskii, and S. A. Firstov, "Two ways of determination of hardness of modern materials by automatic indentation method," in *Electron Microscopy and Hardness of Materials: Collection of Papers* (Kiev, IPM NAN Ukraine, 2008), No. 15, 11–23.
24. X. Liu, M. Q. Zeng, Y. Ma, and M. Zhu, "Melting behavior and the correlation of Sn distribution on hardness in nanostructured Al–Sn alloy," *Mater. Sci. Eng., A* **506**, 1–7 (2009).
25. G. Leibfried, "Microscopic Theory of Mechanical and Thermal Properties of Crystals," in *Handbuch der Physik*, Ed. by S. Flügge, Vol. 7, Part 1 (Springer-Verlag, Berlin, 1955), pp. 104–324.

Translated by T. Gapontseva